Journal of Photochemistry and Photobiology A: Chemistry 222 (2011) 146–158

Contents lists available at ScienceDirect

Journal of Photochemistry and Photobiology A: Chemistry

journal homepage: www.elsevier.com/locate/jphotochem

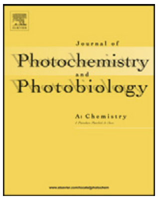

Behavioral features of photostimulated processes in the heterogeneous composition of polymer–semiconductor–salt of a metal

Dmitry S. Shtarev [a,*], Konstantin S. Makarevich [b], Alexander V. Syuy [a]

[a] *Department of Natural Science, Far Eastern State Transport University, 47 Seryshev Street, Khabarovsk 680021, Russia*
[b] *Institute of Material Science Far Eastern Branch of Russian Academy of Sciences, 153 Tihookeanskaya Street, Khabarovsk 680042, Russia*

ARTICLE INFO

Article history:
Received 26 January 2011
Received in revised form 15 May 2011
Accepted 21 May 2011
Available online 27 May 2011

Keywords:
Photostimulated processes
Photocatalysis systems
Polymer photomodifications
Polyene structure formation

ABSTRACT

In the current study experimental data about changes in the photosensitive composition consisting of polyvinyl alcohol, zinc oxide and bismuth chloride (PVA–ZnO–$BiCl_3$) under UV-irradiation are presented. There are both organic (PVA) and inorganic compounds of the named composition whose changes are determined. The main products of the photostimulated reactions are metal bismuth, bismuth oxide and polyene structures of various lengths in the form of a polyvinyl alcohol. In this research a heuristic scheme of photostimulated reactions in the photosensitive composition of PVA–ZnO–$BiCl_3$ and in similar compositions was suggested.

1. Introduction

Processes, occurring in compositions based on different polymers, under irradiation of various spectral ranges, have been investigated by numerous research groups. Such interest is stipulated by the wide spectrum application sphere of similar systems. Systems in which polymer photomodification are observed, find applications in the recording and storage of optical information, lithography and holography [1–4]. Investigating the photoprocesses, occurring in similar compositions during irradiation, has important fundamental meanings such as allowing improved understanding of the electron excitation transfer processes, chemical reaction photoinitiation processes and likewise photomodification processes and photostimulated transformations [5].

Certain photosensitive compositions, of which a detailed review is given as an example in [6], need a developing process after irradiation. However, in other photosensitive compositions the photochemical transformations lead to surface coloration and physical property changes directly during exposure. Such processes are called direct blackening processes. Photosensitive compositions with direct blackening have greater potential for use than compositions which need a further developing process [2,3,7,8]. The present article is devoted to research of the photosensitive composition which consists of polyvinyl alcohol (PVA), zinc oxide (ZnO) and bismuth chloride ($BiCl_3$) [9–11]. It shows photosensitivity to ultraviolet and X-ray radiation. The composition surface coloration is changed under such radiation, i.e. a direct blackening processing occurs [7,8]. This composition can be used for image recording in the UV and X-ray spectral range and as a radiation detector. High sensitivity, fabrication simplicity and image steadiness are its basic distinctions.

Basically photostimulated processes in photosensitive compositions lead to:

(1) Metal phase photoreduction. For example, the PVA–ZnO/TiO_2–$Pb(CH_3COO)_2$ [12,13] composition.
(2) Polymer matrix photostimulated modification. For example, the PVA–$CuCl_2$/$FeCl_3$ [14] composition.

The feature of the PVA–ZnO–$BiCl_3$ photosensitive composition is that most probably both mechanisms have been realized in it [7,8,15]. The behavior of photostimulated reactions in systems of types (1) and (2) is studied in detail [12,13,16–18]. However, these theories do not provide simultaneously metal photoreduction and polymer matrix photomodification. Therefore, it is very important to understand which processes are occurring in the PVA–ZnO–$BiCl_3$ photosensitive composition, at the expense of in which mechanisms the direct blackening processes occur. Besides this principal meaning, understanding the processes will allow us to obtain a composition with preset characteristics (maximal density of blackening, photosensitivity and others). To achieve this aim first of all it is necessary to establish which changes take place in the composition under irradiation.

---

* Corresponding author. Tel.: +7 4212 406375; fax: +7 4212 407321.
E-mail address: shtarev@mail.ru (D.S. Shtarev).

1010-6030/$ – see front matter © 2011 Elsevier B.V. All rights reserved.
doi:10.1016/j.jphotochem.2011.05.014

In a few papers [19,20] it was shown for the first time, that UV-irradiation exposure and UV-irradiation and visible light exposure lead to the formation of different colorations of the PVA–ZnO–$BiCl_3$ composition surface. Meanwhile there are no traceable changes in the composition after irradiation by visible light (only) [19]. The described distinction in the composition surface coloration shows that the formation on the composition surface of such products of the photostimulated reactions may depend on the spectral distribution of the exposure irradiation [20].

Observation of the described effects poses the problem of a more detailed study of the photosensitive composition surface coloration and the spectral distribution of the exposuring irradiation. Solving this task can clarify some behavioral features of photostimulated processes in the photosensitive composition PVA–ZnO–$BiCl_3$.

2. Materials and methods

For the manufacture of the photosensitive composition chemically pure polyvinyl alcohol 11/2 grade, pure zinc oxide and anhydrous, chemically pure bismuth chloride are used.

The photosensitive layer is achieved by the following method: 10 g of the PVA is mixed with 100 g of distilled water and left to draw for up to 10 h. During this time the polyvinyl alcohol granules swell in the water. Then the 10% PVA aqueous solution thus obtained is heated at 80–90 °C for 45 min until the solution becomes homogeneous. After that, 12 g of the zinc oxide is added to 100 ml of the PVA aqueous solution. The resulting compound is mixed up and poured out on to a glass plate. This used no more than 2/3 of the total compound. This means that the heaviest fractions of ZnO were left in the container making the photosensitive composition more homogeneous.

Bismuth chloride unimolar aqueous solution is prepared singly. To make it, 31.5 g of anhydrous bismuth chloride is dissolved in water. Intense hydrolysis takes place during the dissolving. The completely hydrolyzed bismuth chloride – $Bi(OH)_3$ – falls as a white sediment, and the bismuth chloride complexes $BiCl^{3-n}{}_n$ ($n = 0\ldots6$ [21]) basically stay in solution.

After the polyvinyl alcohol filmed with dispersed zinc oxide for 12–15 h drying at normal conditions, the bismuth-containing compound – bismuth chloride aqueous solutions – is added by dipping the filmed bismuth chloride aqueous solutions for 30 s. After that, the surplus moisture is removed from the surface by a warm air flow for 5 min. Measurement shows that as a result of such treatment nearly 9 mass% of the bismuth chloride gets into the photosensitive composition [9].

The exposure of the resulting photosensitive composition was made by mercury-vapor lamp DRT-125 integral light. The energy of UV-irradiation is basically allocated between the spectral ranges: 230–280 nm (9–11%), 280–315 nm (22–25%), 315–400 nm (21–22%). The total luminous flux of the DRT-125 lamp is 1730–1850 lm. The illumination near the photosensitive composition surface during the SEM, TEM, IRS and XPS experiments is 0.105 W/s m^2. The exposure time of photosensitive composition in the SEM, TEM, IRS and XPS experiments is 50 s. Exposure times and illuminances in the diffuse reflectance spectroscopy (DRS) research were changes in ranges, which are presented in Table 1.

The coloration changes of the surface of the PVA–ZnO–$BiCl_3$ photosensitive composition occur under the exposure of DRT-125 with pointed spectral and energetic characteristics shown in Fig. 1. Such changes of surface coloration occur as a result of the series of photostimulated conversions in the volume of composition, which can be ascertained at the expense of such composition structure changes.

Analysis of the structure of the photosensitive composition after exposure has been conducted on the basis of SEM, TEM, IR-spectroscopy and XPS data with the use of the following equipment.

A transmission electron microscope Libra 120 with accelerating potential 80 kV was used for the identification of crystal phases, formed in the direct blackening process.

To obtain complete pattern spectrums of infrared absorption of photosensitive composition before and after exposure, the changes occurring under radiation in polymeric matrix were analyzed. Results were obtained by the use of the IR spectrometer with Fourier transformation “Nicolet-710”.

Analysis of the surface of composition after exposure was made by the XPS method with the Specs high-vacuum plant and SEM with the EVO 40 microscope and the energy dispersion analyzer (EDA). Before the EDA usage the photosensitive composition surface was covered by a gold layer. The remaining experiments would be conducted without additional photosensitive composition surface treatment.

The DRS method was used for determination of the influence of the structure of the exposure irradiation on the product forming. The spectrums of diffuse reflectance were registered using a Specord M40 spectrophotometer in the 230–900 nm spectral range. To make the received experimental data consistent a special cell was produced, which allowed the precision setting of the sample relative to the optical system of the spectrophotometer. Standard optical filters were used to obtain the various spectral distributions of the exposure irradiation.

Three samples were obtained for the analysis of the dependence between the behavior of the photostimulated reactions in composition and the spectral distribution of the exposure irradiation. Its exposure conditions are presented in Table 1.

3. Results

3.1. Scanning electron microscopy

The results received by research on SEM of the surface of the photosensitive layer after exposure are shown in the inserts in Fig. 2 which shows that the surface is coated by globules, forming conglomerations with actual size 1.1–1.3 μm.

The picture of the border between exposed and unexposed parts of the photosensitive composition is presented in Fig. 2. It is shown that the globules are formed under light – on unexposed parts of the composition (Fig. 2 left) globules are practically absent.

Research using an energy dispersion analyzer was carried out for identification of the chemical structure of the photosensitive composition surface after radiation. Fig. 3 shows which areas of the photosensitive composition were explored with EDA. The spectrum from these areas is also presented in Fig. 3. Unmarked peaks in the figure refer to gold, sprayed on the composition before research.

There are bismuth character lines on the spectrum from globules (spectrum 3 in Fig. 3), but they are not on the spectrum from surface without globules (spectrum 4 in Fig. 3). So, from spec-

Table 1
Sample exposure regimes.

Sample No.	The exposure wavelength range	Illumination by the sample surface (mW/s m^2)	Exposure time span (s)
1	303–346 nm	0.718	0–2000
2	365 nm	1.549	0–4000
3	The integral light of the mercury-vapor lamp	105	0–100

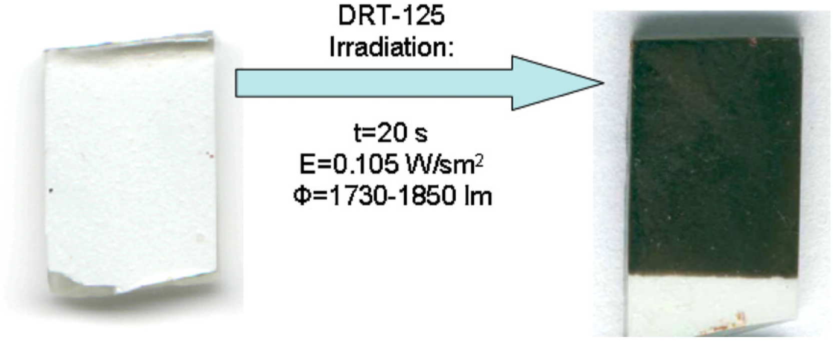

Fig. 1. Photosensitive composition surface coloration changes during the UV-irradiation.

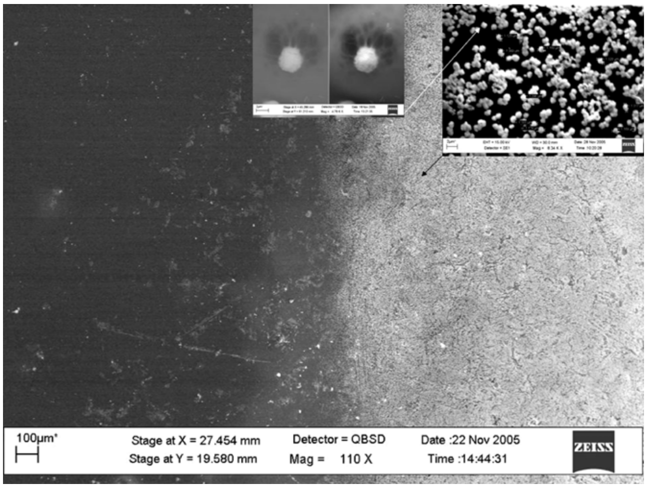

Fig. 2. Picture of the border of an exposed part of composition. Photosensitive composition surface after exposure and single globule are in insert pictures.

trums in Fig. 3 it can be seen: after photosensitive composition UV-irradiation bismuth is presented only in the formed globules. As the globules which contain bismuth are present only on the exposed part of the composition, before UV-irradiation exposure the bismuth-contained compound is practically absent from the photosensitive composition surface.

Thus by the scanning electron microscopy method and EDA research it was established that on the surface of the unexposed PVA–ZnO–$BiCl_3$ composition the bismuth-containing phase is practically absent; the photostimulated processes in photosensitive composition under UV-irradiation lead to the formation of a new bismuth-contained phase on the surface of the photosensitive layer, forming globules with average size 1.1–1.3 µm.

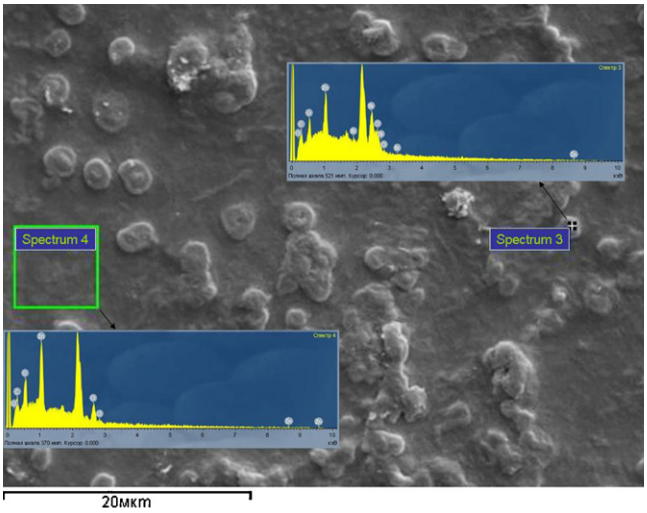

Fig. 3. EDA using areas and EDA spectrum, received from a globule and from surface.

3.2. Transmission electron microscopy

Research using a transmission electron microscope was conducted for the identification of a phase, formed in the volume of composite material under UV irradiation. As the main interest is focused on the photostimulated transformations on surface and near-surface layers in the photosensitive composition, the current experiment explores only surface and near-surface layers of the photosensitive composition. Fig. 4 presents the electron-diffraction

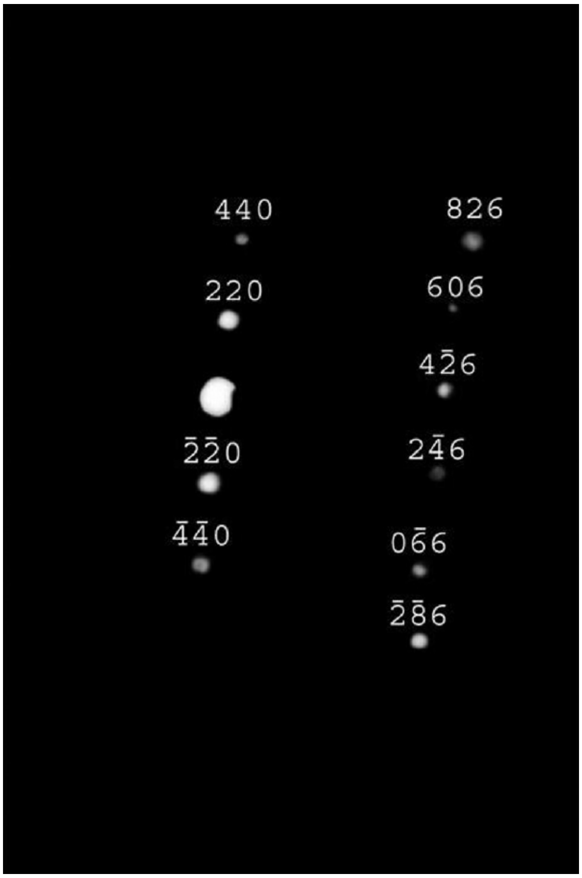

Fig. 4. Electron-diffraction pattern of a composition after exposure. Interplanar spacing corresponds to bismuth oxide.

Table 2
Referencing the experimental data. Interplanar spacing, Å.

Experiment	Etalon ($\mathrm{Bi_2O_3}$)
3.658	3.624
1.735	1.708
1.423	1.45
1.214	1.208
1.070	1.105

pattern of photosensitive composition after exposure. It shows that in the volume of the polymer, having an amorphous structure, crystals are formed with an actual size of nearly 1 μm, which have a point electron diffraction pattern [15]. Reflections of these crystals corresponding to the interplanar spacing, are presented in Table 2. From the table it can be seen that particles forming under UV-irradiating appear to be bismuth oxide monocrystals.

The estimated average size of the particles formed under UV-irradiation was made by the following considerations. As a result of experimental research a point electron diffraction pattern was received. This means that particles which form under UV-irradiating in composition have monocrystal structures. Also it means that these particles have an average diameter no less than the diameter of the electron beam of the transmission electron microscope. During experiment the electron microscope sets were chosen so that the electron beam diameter near the sample surface was approximately 1 μm [22].

This means that changes of the inorganic part of the photosensitive composition (forming bismuth oxide from bismuth-contained compound) occur under light. Thus, on the basis of TEM results a conclusion can be made that the observed photostimulated process has caused the growth in volume of polymeric matrix bismuth oxide crystals.

3.3. Infrared spectroscopy

Changes of the organic part of the photosensitive composition in the exposure process are investigated using infrared spectroscopy.

The spectrum of PVA has three wide bands of absorption in the frequency band: 3590–2814, 1487–1210 and 1152–1010 cm^{-1}, and three closely spaced narrow bands with maximum on 1715, 1662 and 1560 cm^{-1} [23,24]. The presence of clear lines in this part of the spectral range can be correlated with the C=O bond.

So, line 1715 cm^{-1} practically agrees with the well-known line 1714 cm^{-1}, correlated with C=O bond in acetaldehyde structure (HO–C=O). It is known that acetaldehyde is always present in PVA, and this fact is bound with its fabrication technology [23].

The IR-spectrums of the photosensitive composition PVA–ZnO–$\mathrm{BiCl_3}$ were studied before and after exposure. The IR-spectrum of the investigated composition before exposure includes three wide bands of absorption: 3620–2753, 1485–1208 and 1155–1010 cm^{-1}. Besides these bands, the weaker bands in the spectrum are present and they reach their maximum at frequencies 1709, 1655, 1565 and 917 cm^{-1} (Fig. 5). The extremely high absorption of the spectrums presented in Fig. 5 can be explained by the significant thickness of the photosensitive composition (about 1 mm). A change in the low-frequency part of the IR-spectrum (inserts in Fig. 5) appears after exposing the composition for 50 s under ultraviolet irradiation.

So, the intensity of the band of absorption with a maximum at frequency 917 cm^{-1} has decreased, but bands of absorption at frequency range 892–906 and 926 cm^{-1} have appeared. The appearance of this band of absorption most probably indicates the modification of polyvinyl alcohol – appearance in its structure $\mathrm{CR^1R^2{=}CH_2}$ groups. In addition an increase in absorption of three lines in range 1715–1565 cm^{-1} is observed.

The line of absorption 1715 cm^{-1} was previously identified as corresponding to C=O vibration in acetaldehyde. The two other lines shown in inserts in Fig. 5 are located in the area of C–O and C=O vibration bonds. It is impossible to identify these lines more accurately using this method.

Thus by IR-spectroscopy research it was identified that the UV-irradiation influence on the PVA–ZnO–$\mathrm{BiCl_3}$ photosensitive composition led to the polymer matrix modifications. In particular the polymer modification with formation of the C=O double

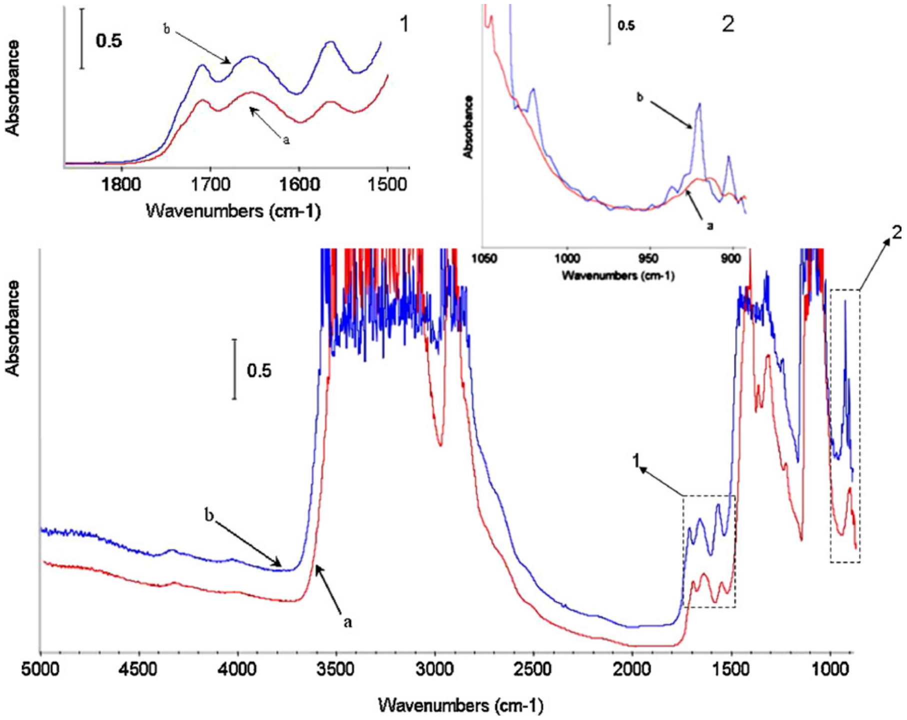

Fig. 5. IR-spectrum of PVA–ZnO–$\mathrm{BiCl_3}$ composition before (a) and after (b) exposure. Low-frequency parts of composition IR-spectrum are in the inserts.

bond and $CR^1R^2{=}CH_2$ groups in the photosensitive composition PVA–ZnO–$BiCl_3$ under UV-irradiation was established. Also the presence of vibrations in the IR-spectrum stipulated by the presence of acetaldehyde was determined.

3.4. X-ray photoelectron spectroscopy

The surface of the photosensitive composition after exposure was studied by the X-ray photoelectron spectroscopy method (XPS). The selected research method allows determining both the elements located on the sample surface and other compounds generated by these elements [25–27]. The spectrum of the photosensitive composition surface after exposure to UV-irradiation is presented in Fig. 6. The character peaks of all elements included in the composition (zinc, oxygen, carbon, bismuth, and chlorine) are marked on the spectrum. Allocation of the mentioned elements on the photosensitive material surface is also given in Fig. 6. As the targets of research are defining changes in the composition structure under UV-irradiation, bismuth and carbon lines require more thorough research.

As can be seen from Fig. 6a, the carbon line in the spectrum is complex and well-described by four Gaussians with following maximum positions: A – 284.49 eV, B – 285.09 eV, C – 286.08 eV, D – 289.02 eV. The obtained experimental data can be interpreted in the following way.

The B-line relates to carbon ingression of PVA (a linear carbon chain without double bonds in the capacity of radical atoms of hydrogen and OH– groups appears) [26]. Shifted by 0.6 eV against the basis line A (284.49) eV corresponds to a linear carbon chain with alternate double and single bonds (–C=C–C=C–) [26]. Such a form of carbon chain is called a polyene structure. In a number of sources [14,18] blackening, incipient in such photomaterials, is associated with the formation of polyene structures in it. The D-line whose amplitude is considerably lower than that of other lines, shifted against the carbon standard line (285 eV) by 4 eV. Such strong shifting is typical of carbon in the structure of acetaldehyde (HO–C=O) [26]. The C-line, shifting to the side of higher energy by 1 eV against the B-line, can be referred to C–O–C or C–O–C=O bonds. The existence of such bonds in the polymer structure after exposure is evidence of intermolecular cross-linking. So, the C–O–C bond can be generated as a result of the cross-linking of two polymer molecules and the C–O–C=O bond can be generated as a result of the cross-linking between PVA and acetaldehyde molecules.

Table 3
Referencing the experimental data.

Compound type	Bi $4f_{7/2}$ binding energy (eV)	
	Experiment	Etalon [27]
Bi	157.8	157.0
Bi_2O_3	159.28	159.2–159.8

Bismuth doublet $4f_{5/2}$ and $4f_{7/2}$ lines are presented in Fig. 6b. Each of them consists of two closely spaced lines, with amplitude ratio 1:3. The maximum of the A-line is observed at 157.8 eV, the maximum of the B-line – at 159.28 eV (Table 3). The A-line corresponds to the metal bismuth, whereas the B-line is shifted to the high energy area by nearly 1.5 eV. Such shifting of the maximum occurs in cases, when elements are present on the sample surface in oxide form [27] (Table 3). It allows us to conclude that formation of the metal bismuth and bismuth oxide from its chloride

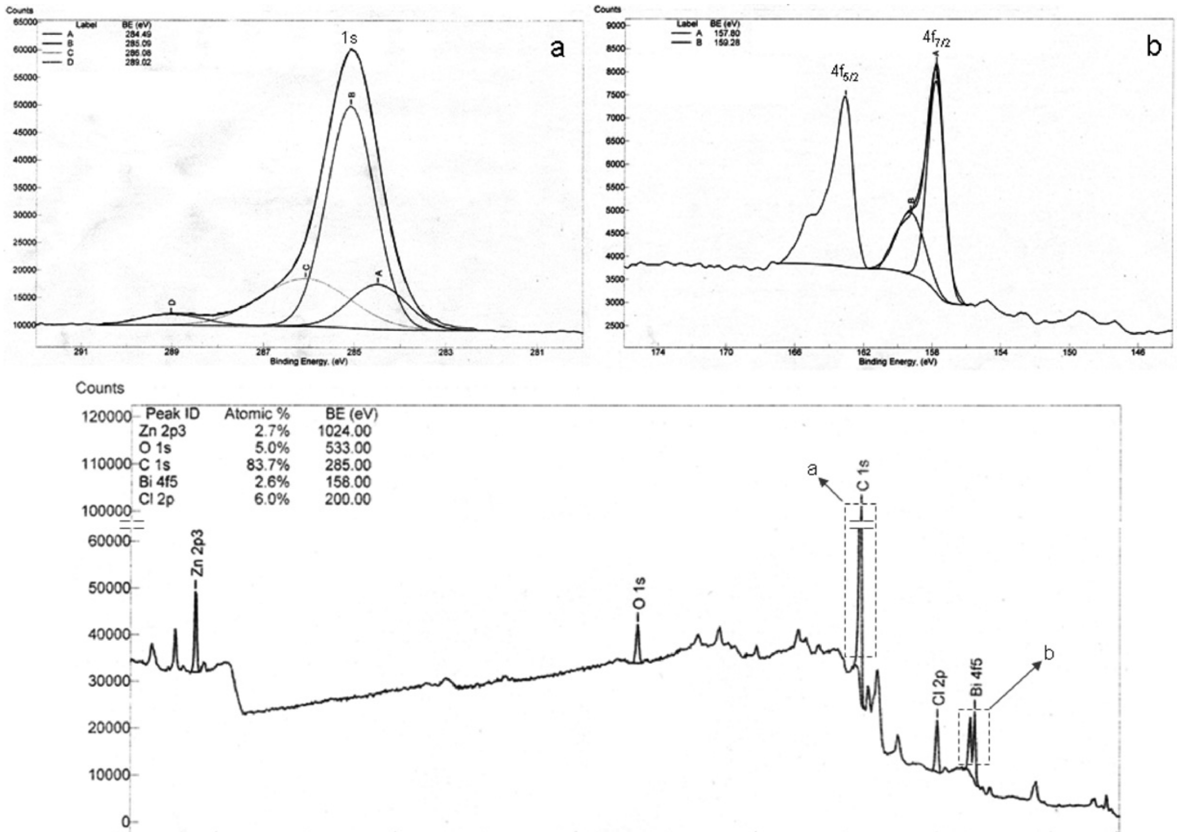

Label	BE (eV)
A	284.49
B	285.09
C	286.08
D	289.02

Label	BE (eV)
A	157.80
B	159.28

Peak ID	Atomic %	BE (eV)
Zn 2p3	2.7%	1024.00
O 1s	5.0%	533.00
C 1s	83.7%	285.00
Bi 4f5	2.6%	158.00
Cl 2p	6.0%	200.00

Fig. 6. The XPS spectrum of PVA–ZnO–$BiCl_3$ composition after exposure. (a) Carbon line in XPS spectrum of PVA–ZnO–$BiCl_3$ composition after exposure and (b) bismuth line in XPS spectrum of PVA–ZnO–$BiCl_3$ composition after exposure.

occurs in the photosensitive composition under ultraviolet radiation. The formation of bismuth oxide agrees well with TEM-data. XPS research allows us to make the following conclusions.

Under ultraviolet radiation the structure of the polymer matrix in a photosensitive composition is modified. Along with the source linear carbon chains after exposure in polymer structure conjugated single-double bonds appear, to all appearances causing the stipulated blackening. In addition a result was observed which allows us to suppose the formation of intermolecular cross-linking between single molecules of PVA and between molecules of PVA and acetaldehyde. Experimental data also confirm the presence of acetaldehyde in composition.

The inorganic part of photosensitive composition also changes. The received data allow us to claim that the formation of the metal bismuth and its oxide from source bismuth chloride happens in photosensitive composition under ultraviolet irradiation.

3.5. Diffuse reflectance spectroscopy

The influence of the various spectral range irradiations on the photosensitive composition PVA–ZnO–$BiCl_3$ leads to the formation of different colorations of the composition surface. These differences are clearly shown in the diffuse reflectance spectrums (Fig. 7). In all the exposure regimes described above (Samples Nos. 1–3) three absorption bands with well-marked maximums are observed. Every exposure regime has its own characteristic rate of increase of absorption bands. Contention spectrums in Fig. 7a–c show that changing the spectral distribution of the exposure irradiation also changes the positions of the absorption band maximums.

Further analysis of the received experimental data array was made in two basic directions:

- dependence of the positions of the absorption band maximums from the spectral distribution of the exposure irradiation;
- estimation of the kinetic and enthalpy characteristics of the photostimulated processes in PVA–ZnO–$BiCl_3$ photosensitive composition.

Exposure of the Sample No. 1 (Fig. 7b) leads to increased intensity of the absorption band with maximums on 411 nm, 535 nm and 676 nm; exposure of the Sample No. 2 (Fig. 7c) leads to increased intensity of the absorption band with maximums on 417 nm, 493 nm and 554 nm; exposure of the Sample No. 3 (Fig. 7a) leads to increased intensity of the absorption band with maximums on 417 nm, 478 nm and 554 nm. The shifting of the positions of the absorption band maximums subject to exposure regime is shown in Fig. 8. The following regularity can be seen: the higher energy of the exposure photons leads to the formation of the absorption band in the long-wavelength part of the spectrum. It is well known that polyene structures have similar properties [28]. Nor-

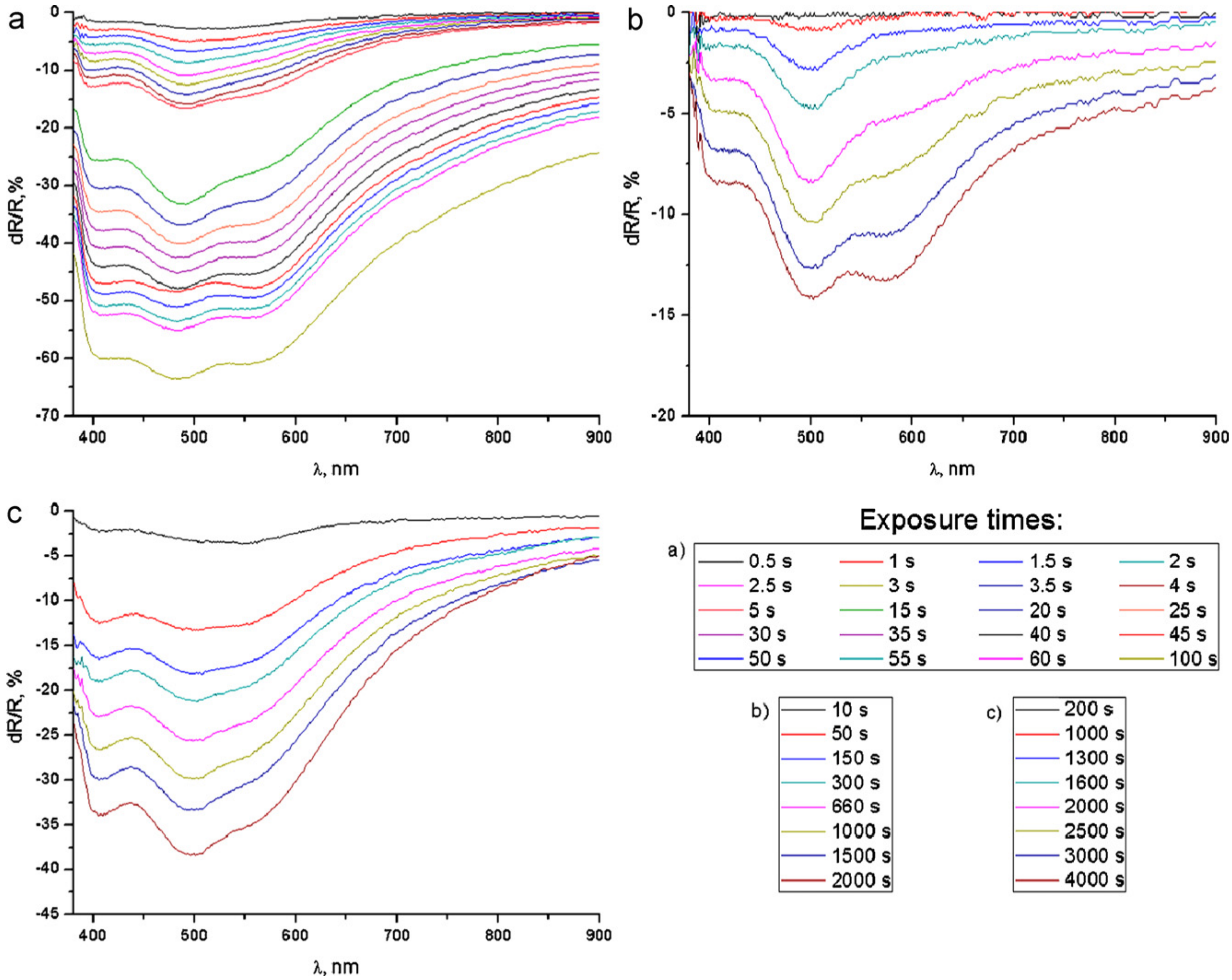

Fig. 7. The changes in the diffuse reflectance spectrums under Photosensitive composition PVA–ZnO–$BiCl_3$ exposure: (a) by the mercury-vapor lamp integral light; (b) by the 303–346 nm spectral range of the mercury-vapor lamp light; and (c) by the 365 nm spectral line of the mercury-vapor lamp light.

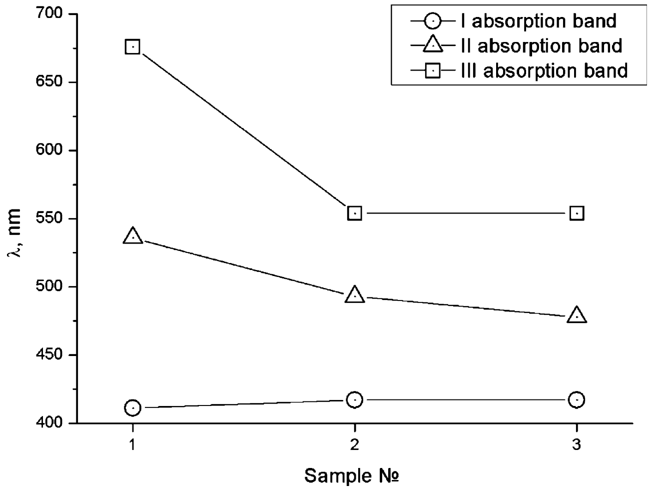

Fig. 8. The position of the absorption band maximums by the different exposure regimes.

mally carbon–carbon double bonds which are not conjugated or only conjugated with only one or two other carbon–carbon double bonds have high enough energy that they absorb in the ultraviolet region of a spectrum, but the absorption energy state of polyenes with numerous conjugated double bonds can be lowered such that they enter the visible region of the spectrum, resulting in compounds which are colored yellow or other colors. Finding regularity (Fig. 8) can provide evidence that more short-wavelength (303–346 nm) UV exposure of the composition leads to the formation of more extensive chains of conjugated carbon–carbon double bonds $(\text{–C=C–C=C–})_n$.

The positions of the maximums of the absorption bands for all exposure regimes (Fig. 7a–c) do not change during increase in exposure time. This means that the length of the formed polyene structures does not depend on the exposure time [29,30].

The intensity of each described absorption bands increased with proper rate under photosensitive composition exposure. The kinetic curves of the intensity of absorption bands (*dR*/*R*, %) increases at various exposure regimes in depend once on exposition (*H*, W*s/s m^2) presented in Fig. 9. As a characteristic, which indicates the intensity of the absorption band rate (*dR*/*R*), the attitude of the change of the diffuse absorption factor to the diffuse absorption factor of the unexposed sample (*R*) was used. On the abscissa axis of Fig. 9 it was laid off exposition (*H*, W*s/s m^2) of the photosensitive composition, which are products of exposure time (τ, s) on the illumination (*E*, W/s m^2) under photosensitive composition surface. This characteristic was chosen because similar photochemical transformations can occur in photosensitive composition as a result of both short impact of high-powered irradiation and the prolonged impact of low-powered irradiation.

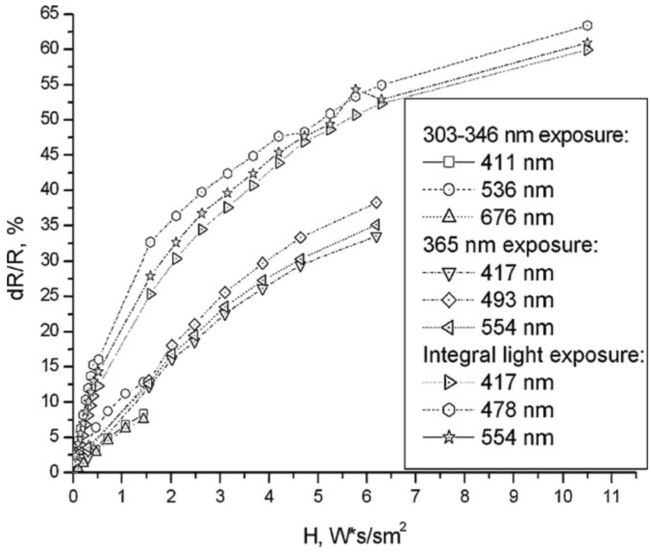

Fig. 9. A kinetic curve of the absorption band intensity growth in the different exposure regimes.

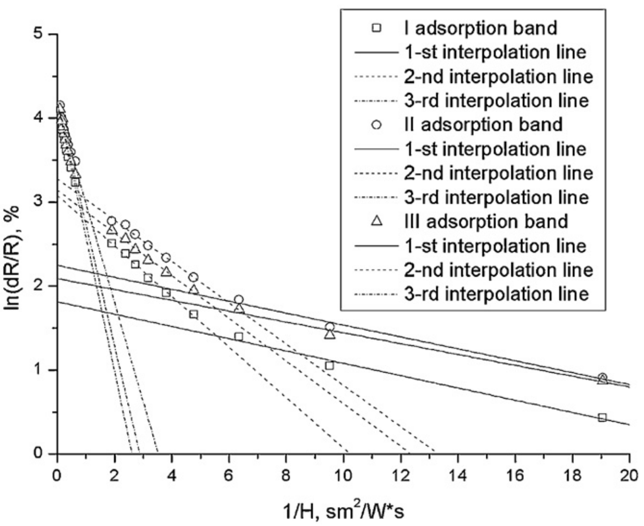

Fig. 10. The process of the absorption band intensity growth in the photosensitive composition under integral light of the mercury-vapor lamp exposure.

From Fig. 9 one can see that the rate of increase of intensity of the absorption bands is basically determined by the wavelength of the exposure light. The curve character of the intensity of absorption band rate in all exposure regimes is practically identical. The highest rate of increase of intensity of the absorption band was observed under exposure using the integral light of the mercury-vapor lamp.

The absorption bands arising from exposure to the photosensitive composition surface characterize a specific product of the photochemical transformation, which absorbs a certain wavelength range. These product formations are characterized by a specified enthalpy of the process – enthalpy of irreversible chemical reactions (including photochemical transformations in the considered system) or properties that are difficult to be accessed by the use of traditional thermodynamic techniques. However, recent developments of several types of spectroscopic methods enable us to measure these quantities for a variety of irreversible reactions [31]. As a characteristic, which gives information about enthalpy of the photochemical processes the slope of the kinetic curves plotted in ln(*dR*/*R*) and 1/*H* coordinates may be used [32,33]. In Fig. 10 by this method the kinetic curves for integral light exposure of the photosensitive composition are plotted. On the presented graphics three consistently changed linear sections with character tilt angles can be marked out. Similar areas with character tilt angles can be marked out after analysis of the experimental data of the other exposure regimes (303–346 nm and 365 nm). The presence of such features indicates that there are thee conjugated photochemical reactions occurring in the photosensitive composition PVA–ZnO–BiCl$_3$ and each of them is characterized by its own enthalpy.

4. Discussion

Based on the research and received experimental data the following heuristic mechanism of photostimulated processes in heterogonous composition PVA–ZnO–BiCl$_3$ can be offered.

In the composition considered, light in the ultraviolet range is absorbed both by polyvinyl alcohol and by zinc oxide. The formation of photoelectrons (e_f) and photoholes (O_S^-) is the result of zinc oxide photoexcitation.

In heterogeneous mechanism of photocatalysis [34], when molecule like RH participates in the next reaction near the photohole is well-known:

$$HR + O^-{}_S \rightarrow O_SH + R^\bullet \quad (1)$$

Water molecules, which assist in the composition (for example, forming in the destruction of hydroxide bismuth micelle) near zinc oxide photoholes can also participate in the interaction (1):

$$HOH + O^-{}_S \rightarrow O_S + OH^\bullet \quad (2)$$

The O_S^- photoholes are formed on the zinc oxide surface as a result of photosensitive composition UV irradiation [35–37]. As a result of the reaction (2) the hydrogen-radical associates with photoholes on the zinc oxide surface, but another hydroxide-radical is available relatively free.

This hydroxide-radical can attack certain carbon atoms in the PVA chain by the following scheme (Fig. 11a) [38–40]. At this stage there is the initiation step of the radical substitution mechanism. Such reaction becomes possible thanks to the oxygen atoms in the PVA structure which draw off part of the electron density from the carbon atoms. As a consequence some carbon atoms in PVA get positive potential $+\delta$ and these particular atoms will be attached by hydroxide-radicals [40]. The radical of hydrogen and monomer of PVA with two hydroxyl groups by one carbon atom is the result of such a process. This structure is unstable so it reforms water and the monomer (CH_2–C=O) [38].

The formation of C=O bonds under irradiation is confirmed by IR-spectroscopy and XPS data. The next cycle of circumscribed reactions can be initialized by the water arising.

Previous research [8,10] shows that in the course of the preparation of the photosensitive composition the bismuth oxychloride BiOCl [41] is produced on its surface. This happens because impregnation of the polymer matrix is made by an aqueous solution of bismuth chloride, with active hydrolyzation by the following reaction [42]:

$$BiCl_3 + H_2O \rightarrow 2HCl + BiOCl^\bullet \quad (3)$$

The hydrogen-radical, generated by the scheme in Fig. 11a can initiate the bismuth and bismuth oxide reduction from its oxychloride with the release of hydrochloric acid.

At the first stage, atomic hydrogen tears from the bismuth oxychloride atom of the chlorine with the formation of hydrochloric acid:

$$BiOCl + H^\bullet \rightarrow HCl + BiO^\bullet \quad (4)$$

Such a reaction is possible, because chlorine atoms in the bismuth oxychloride crystal are considerably distant from bismuth atoms and weakly bound with them [42]. As a result bismuthile is formed. In a number of sources (for example [21]) it is shown that bismuthile (BiO) is unstable and at the second stage it tends to pass to a stable form – BiO(OH) – at the expense of capturing the hydroxide-radical, which is formed in reaction (2):

$$BiO^\bullet + OH^\bullet \rightarrow BiO(OH) \quad (5)$$

After that the received bismuth hydroxide dehydrates and bismuth oxide is formed [43]:

$$2BiO(OH) \rightarrow Bi_2O_3 + H_2O \quad (6)$$

TEM and XPS experimental data do confirm the formation of bismuth oxide as one of the ultimate products of photostimulated processes in composition. Schematically, the processes of forming bismuth oxide can be presented by the following mode (Fig. 11b).

Photoelectrons, formed in photoexcitation of ZnO, can reduce bismuth to the metal state from any bismuth-containing compound, which is shown in Fig. 11. The presence of the metal bismuth on the composition surface after exposure is confirmed by XPS experimental data. Photoreducted metal bismuth colors the composition surface. At this stage a visible image is generated at the expense of the formation of metal bismuth on exposed parts.

Hydrochloric acid molecules formed in reaction (4) appear as catalysts of dehydrogenation and dehydration reactions of PVA [44]. Alternate double bonds C=C are generated in PVA in places of abruptions of hydrogen and hydroxyl groups (Fig. 11c) [44].

These alternate single and double bonds (Fig. 11c) are called polyene structure. In their turn, all polyene structures adsorb visible light, i.e. appear colored [45,46]. IR-spectroscopy and XPS experimental data do confirm the formation of polyene structures in PVA–ZnO–$BiCl_3$ composition. At this stage a visible image at the expense of modification of polymer matrix on exposed parts is generated.

The DRS experimental researches allow us to complement and to specify the suggested mechanism of photostimulated processes. The formation and growth of the polyene structures in the volume of a PVA can occur:by the formation of double bonds in areas of PVA molecules directly abutted on an already arising polyene structure;by the parallel and simultaneous growth of polyene structures of a similar length in different parts of PVA molecules.The formation of polyene structures by (a) model would be accompanied by the shifting of the maximums of the absorption bands in the DRS spectrums [29,30], which are not observed in experiment. Also the polyene structure growth by (a) model should be accompanied by the continuous increase of the activation energy as a result of an increasing energy barrier between the forming polyene structure and the ambient PVA molecule [29,51]. Hence the parallel formation of similar length polyene structures (b model) is the more energy-optimal model. Thus in all probability it could be said that the formation of similar length polyene structures under the influence of UV-irradiation on the photosensitive composition surface occurs. This is confirmed by the increase in the intensity of all absorption bands without the shifting of the positions of the maximums.

At the same time it was shown that more short-wavelength exposure shifts the positions of the absorption bands maximums to longer wavelength spectral range. This is evident that more short-wavelength radiation initiates the formation of longer polyene structures.

The wavelength of the exposure irradiation determines the maximum length of the polyene structure forming as a result of the photostimulated processes, while the illumination and exposure times determine the amount of the polyene structure on the composition surface.

On the kinetic curves of the increase of the absorption bands plotted in $\ln(dR/R)$ and $1/H$ (Fig. 10) coordinates three linear sections with the characteristic tilt angles can be marked out. The presence of such features indicates that there are three conjugated photochemical reactions which occur in the photosensitive composition PVA–ZnO–$BiCl_3$ and each of them is characterized by its own enthalpy. In all likelihood the stages correlate with:

(a) the different forming stages of the polyene structures;
(b) the different localizations of the areas of formation of the polyene structures in the PVA molecules (near the edge of the PVA molecule, near the structural defects in the PVA molecule, on the defectless area of the PVA molecule).

In [29] it is shown that the wavelength position of the maximum of the absorption band is linearly dependent on the number of the

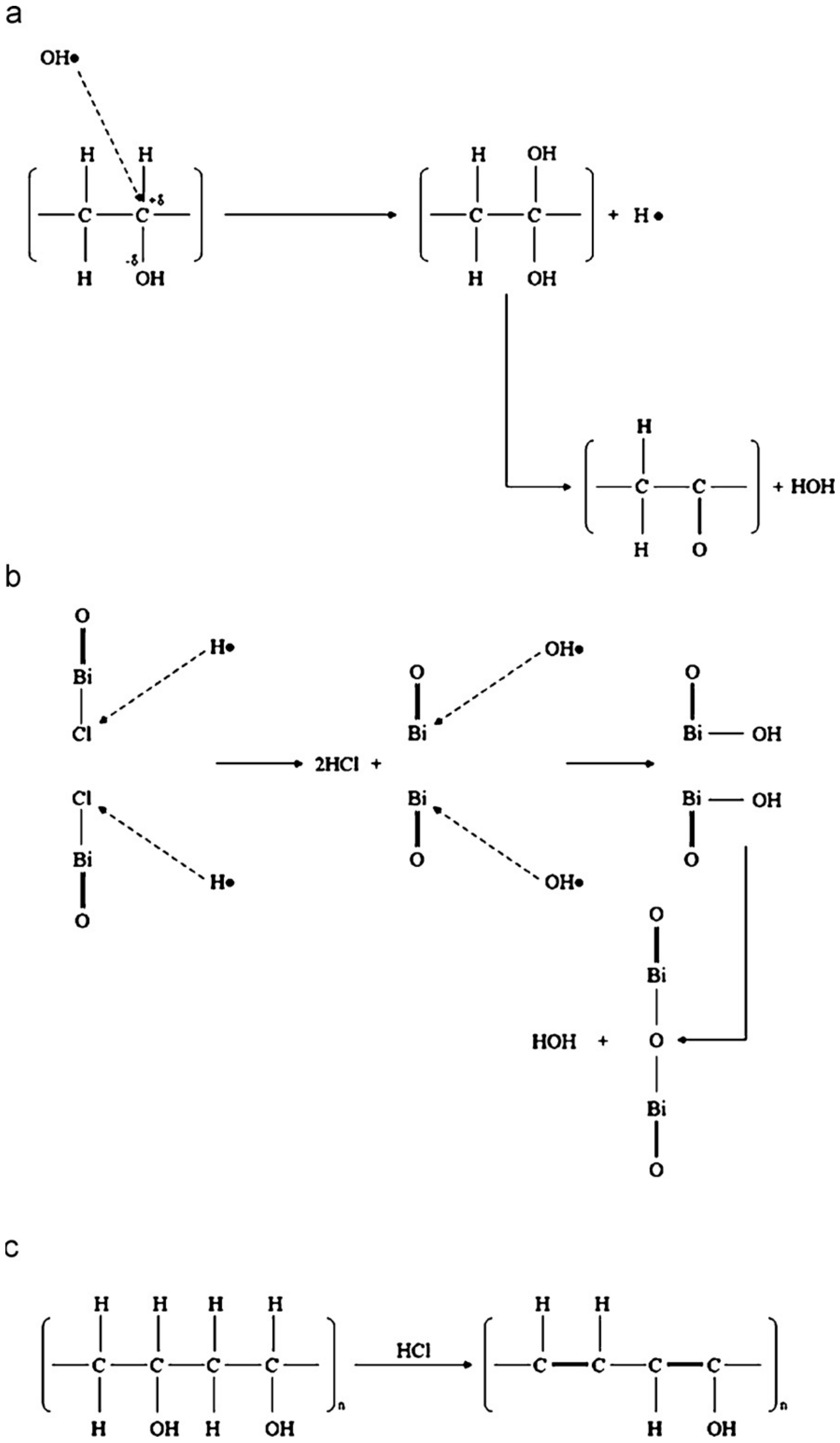

Fig. 11. Scheme of photostimulated processes. (a) Scheme of attack of PVA by hydroxyl-radical, (b) scheme of bismuth oxide formation, and (c) scheme of polyene structure formation in PVA.

conjugated bonds in the polyene structure and can be found from the equation:

$$\lambda \sim (2n+1)d, \qquad (7)$$

where λ is the maximum absorption band; *n* is the number of the conjugated double-single carbon bonds; and *d* is the C=C bond distance.

But experimental research shows a deviation from the linearity (Fig. 12, [29,47]), which is explained by the shortening of the C=C bond distance due to the growth of the polyene structure [48]. By comparing the literature (Fig. 12, [29,47]) and experimental data on the positions of the maximum of the absorption bands the number of the conjugated C=C bonds, forming in the photosensitive PVA–ZnO–$BiCl_3$ composition under various exposure regimes (Table 4) can be determined. From the table it is obvious that the influence of the shorter wavelength UV irradiation leads to more extensive polyene structure formation (up to 22 C=C conjugated bonds). Altogether such a conclusion was already formulated above but on the basis of other reasons.

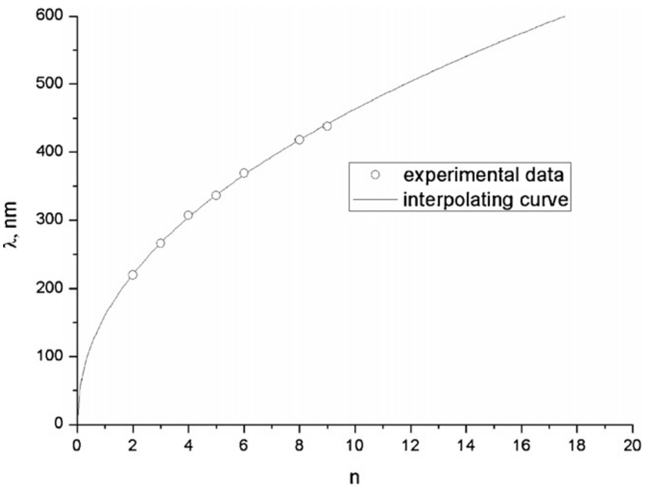

Fig. 12. The dependence of the long-wave absorption band position by the number of conjugated bonds in the dimethylpolyene [29,47].

Table 4
Number of the conjugated bonds in the polyene structures, forming in the photosensitive composition depending on the exposure regimes.

Sample No.	The exposure wavelength range	Maximum of the absorption band (nm)	Number of the conjugated bonds in the forming polyene structure
1	303–346 nm	411	7–8
		536	13–14
		676	22–23
2	365 nm	417	7–8
		493	11–12
		554	14–15
3	The integral light of the mercury-vapor lamp	417	7–8
		478	10–11
		554	14–15

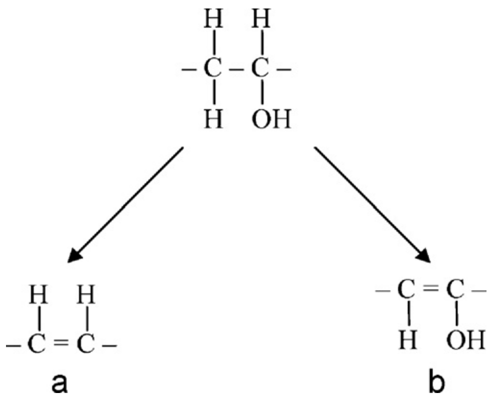

Fig. 13. The scheme of the competing reactions of the double bond forming in the PVA.

Table 5
The elemental composition of the PVA–ZnO–BiCl$_3$ photosensitive composition surface.

Element	Concentration (at.%)	Binding energy (eV)
Zn 2p3	2.7	1024.0
O 1s	5.0	533.0
C 1s	83.7	285.0
Bi 4f5	2.6	158.0
Cl 2p	7.0	200.0

For the exploration of the direct blackening processes, occurring in the PVA–ZnO–BiCl$_3$ photosensitive composition, the model in which one of the ultimate products of the photostimulated reactions are polyene structures $(-C{=}C-C{=}C-)_n$ with the conjugated bonds ranging from 8 to 23 was suggested. Formation of the double bonds C=C occurs as a result of the dehydrogenation and dehydration reactions. This formation of the double bonds can occur by one of the two ways, which are shown in Fig. 13 [52]: at the expense of removal of the hydrogen atom and the hydroxyl group ("type A" reaction, Fig. 13a) or at the expense of removal of the two hydrogen atoms ("type B" reaction, Fig. 13b).

From Fig. 13 it can be seen that initial base unit of the PVA molecule and the final products presented in Fig. 13a and b are characterized by various carbon and oxygen specific contents:

- *initial base unit of the PVA molecule*: there are two carbon atoms on one oxygen atom;
- *double bond forming in the "type A" reaction*: only 2 carbon atoms are present, oxygen atoms are absent;
- *double bond forming in the "type A" reaction*: there are two carbon atoms on one oxygen atom.

It enables to know the distribution elements on the photosensitive composition surface after exposure, to determine the ratio between the intensities of the two concurrent reactions behavior which are present in Fig. 13. To make this it is necessary to determine the ratio between the n and m value in Eq. (8) so that they satisfy the experimental data about distribution of the elements on the composition surface.

$$\frac{2n+2m}{n}=\frac{K_C}{K_O} \tag{8}$$

In Eq. (8) m and n are quantity of reactions occurred by "type A" and "type B" reactions, respectively; K_C, K_O are specific weight of a carbon and oxygen on the PVA–ZnO–BiCl$_3$ photosensitive composition surface after exposure (in at.%).

In Table 5 advance a data about photosensitive composition compound after its exposure by the integral light of the DRT-125 mercury-vapor lamp during 50 s. The data were received by XPS method with the Specs high-vacuum plant (Section 3.4).

It is necessary to consider that zinc on the photosensitive composition surface (2.7 at.%) is attended only in the oxide form (ZnO). So, the ratio between carbon and oxygen atoms in the photomodified PVA molecules differed somewhat from the tabular value and presents the value: $K_C/K_O = 83.7/2.3$. After substitution of the received value into Eq. (8) it can be obtained:

$$\frac{2n+2m}{n}=36.39 \Rightarrow m=17.195n \tag{9}$$

Thus, to supply the experimental observed ratio between carbon and oxygen atoms in the photomodified PVA molecules it is necessary that the 17 "type A" C=C double bond forming reactions are the share of each one "type B" C=C double bond forming reaction.

This result well agrees with the high-molecular compound chemistry general representation [52,53]. It is well known that structure forms in the "type B" reaction are possible, but extremely unstable and because keto-enol tautomerism are reforms (Fig. 14, [53]) with the aldoxime-group formation and C=C double bond breaking.

The obtained ratio between the intensities of the competitive processes of the forming double bonds in the PVA (17:1) and making observations about the behavioral features of the "type B" reaction allows to make a numerical simulation of the polymer modification process and to identify the most probable lengths of

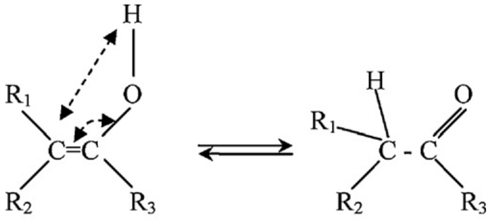

Fig. 14. The scheme of the keto-enol tautomerism in the PVA modified by the “type B” double bond.

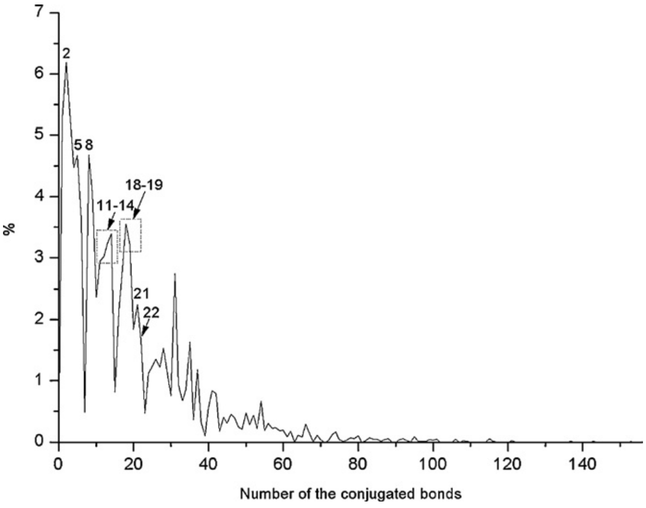

Fig. 16. The length distribution of the forming polyene structures. The numbers over the graph – lengths of the polyene structures whose forming in the describe condition are the most preferable.

the arising polyene structures. The simulation was realized on the basis of the following initial conditions:

- the probability of the “type A” reaction are in range from 0.72222 to 0.94444;
- the probability of the “type B” reaction is $p(\mathrm{B}) = 1 - p(\mathrm{A})$;
- the formation of the double bonds in the “type B” reaction lead to breaking the polyene structure growth in the result of the keto-enol tautomerization;
- the simulation was realized for the double bond formation in the 250 PVA molecules each of which has the 3600° of polymerization. Integrally it was simulated a modifications in the 900,000 of the PVA base unit.

In Fig. 15 the results of the numerical simulation of the PVA modification at different probabilities of the “type A” reaction are present. From the figure it is obvious that the length distributions of the forming polyene structures are substantially determined by the $p(\mathrm{A})$ probability. The higher the probability of the competing reaction (“type B”), the more often the breaking of the polyene structure growth occurs. From Fig. 15 it is obvious that at the low probabilities of the “type A” reaction (graphs 1–6) in the volume of the polymer only short polyene structures arise and the number of the conjugated bonds is at most 10–15.

At the increasing of the probability of the photostimulated modification due to “type A” process situation are changes: along with the short polyene structures ratio decreases there part of the longer polyene structures (with the number of the conjugated bonds to 60) have been increase and the vary long polyene structure with the number of the conjugated bonds to 150 have been appear. From the research it is understood that under described exposure regime the probabilities of the $p(\mathrm{A})$ and $p(\mathrm{B})$ are, respectively, equal 0.9444(4) and 0.0555(5). The polyene structure length distribution which is corresponding to the pointed probabilities of the competing reaction leaking is present in Figs. 15 (graph 10) and 16.

From Fig. 16 it can be seen that the length distribution of the forming on the photosensitive composition surface polyene structures is not steady. Such pictures are usual for the radical polymerization mechanism [52]. There is certain length of the polyene structure whose formation due to described photostimulated processes is more preferable.

Previously by the DRS method (Section 3.5) it was found that the polyene structures of the defined length forms depend on the chosen exposure regime (exposure wavelength). Its comparison with the numerical simulation results is present in Table 6. From the table it is obvious that there is close fit between experiment and numerical simulation: all polyene structures forming as a result of the photostimulated processes are most likely from the point of view of the PVA modification numerical simulation.

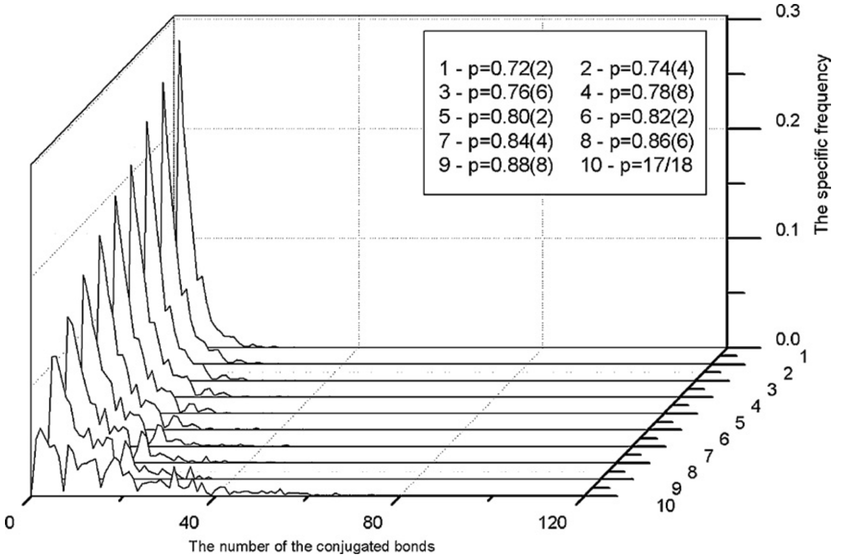

Fig. 15. The length distribution of the polyene structures forming in the volume of the PVA. The probabilities of the double bond forming as a result of the “type A” reaction are in the insert picture.

Table 6
The comparison of the DRS results and numerical simulation.

Sample No.	The exposure wavelength range	Maximum of the absorption band (nm)	Number of the conjugated bonds in the forming polyene structure	The most probable polyene structure length	Ratio of these polyene structure (%)
1	303–346 nm	411	7–8	8	37
		536	13–14	13–14	48
		676	22–23	21–22	15
2	365 nm	417	7–8	8	34
		493	11–12	11–12	39
		554	14–15	14	27
3	The integral light of the mercury-vapor lamp	417	7–8	8	35
		478	10–11	11	36
		554	14–15	14	29

From the length distribution of polyene structure represented in bar chart (Fig. 16) it is possible to make a quantitatively evaluation of the ratios of the different length polyene structures whose forming is on the photosensitive composition surface under UV-exposure (Table 6).

The numerical simulation of the PVA photomodification processes shows (Fig. 16) that the probabilities of the concurrent reactions of the double bond formation (Fig. 13) have a profound influence on the length of the forming polyene structures. One of the ways to improve the duration of the forming polyene structures is to decrease the probability of the double bond forms in the “type B” process breakage (Fig. 14), i.e. stabilization of the enol form of the compound. There are many experimental data in the science literature about stabilization of the enol form in the keto-enol tautomerism, for example by the substitution electrophilic unimolecular reactions [54]. However, applicability of the such method for the PVA–ZnO–$BiCl_3$ photosensitive composition needs further research.

5. Conclusions

In this article experimental data are presented on the UV-irradiation induced PVA–ZnO–$BiCl_3$ photosensitive composition changes. Modification of both organic (the PVA matrix) and inorganic (bismuth chloride) parts of the composition was found. The principal possibility of the photosensitive composition with direct blackening processes with simultaneous organic–inorganic modification production is shown.

The following role of the separate parts of the photosensitive composition can be offered if the proposed scheme is accepted. Adsorbing the UV-irradiation the zinc oxide photoexiting produced photoelectrons and photoholes, needed for the next stage of the photostimulated modifications. At this stage quite a number of photostimulated reactions (such as reactions in Fig. 7) occur on the photosensitive compositions layer (forming the apparent coloration changes, Fig. 1) with significant spacing (to 0.1 mm, [9]) from the zinc oxide. This means that in the example of the PVA–ZnO–$BiCl_3$ photosensitive composition not only complex photostimulated reactions, but also the energy transfer process from excitation areas (zinc oxide particles) to chemical reaction behavior areas (composition surface) can be studied.

It was shown that spectral distribution of the exposure irradiation could substantially influence both the rate of occurrence of the photostimulation reaction and the length of the polyene structures, which are one of the ultimate products of the photostimulated transformations.

The obtained result indicates that the apparent image on the photosensitive composition surface forms during direct blackening processes both by metal bismuth and bismuth oxide produces and by polyene structures in the formation of PVA. This is atypical for similar systems too. All these features make the PVA–ZnO–$BiCl_3$ photosensitive composition unique and promising for further research. In particular the most promising line seems the conductive of photosensitive compositions after UV-irradiation measures. Such research can discover new fields of application of similar systems, inasmuch as it is well known that polyene structure, forming due to PVA modification [49] is able to have a considerable electron conduction [50,51].

References

[1] B. Ranby, W.T. Yang, O.N. Tretinnikov, V. Tokarev, Y.H. Xu, Lamination of polymer films by bulk surface photografting process and properties, Chinese Journal of Polymer Science 19 (2) (2001) 123–127.
[2] M. Itoh, et al., Journal of Physics D: Applied Physics 31 (1998) 463.
[3] Y.S. Cha, M. Tsunooka, H. Makoto Tanaka, H. Konishi, Journal of Applied Polymer Science 29 (2003), 2941.
[4] Photopolymerization type photosensitive lithographic printing plate precursor, United States Patent 7767380.
[5] X. Zhanga, Z.-C. Li, K.-B. Li, S. Lin, F.-S. Du, F.-M. Li, Donor/acceptor vinyl monomers and their polymers: synthesis, photochemical and photophysical behavior, Progress in Polymer Science 31 (10) (2006) 893–948.
[6] K.I. Jacobson, R.E. Jacobson, Imaging Systems, Focal Press, London, 1976, 317 p.
[7] D.S. Shtarev, K.S. Makarevich, V.N. Brui, I.Yu. Prosanov, Photographic materials with direct blackening based on polymer–semiconductor compositions, Proceedings of SPIE 5851 (405) (2005).
[8] D.S. Shtarev, I.Yu. Prosanov, A.A. Tsiganenko, Research of photoprocesses in compositions of the polymer–semiconductor, Proceedings of SPIE 6595 (2007) 18.
[9] I.Yu. Prosanov, D.S. Shtarev, K.S. Makarevich, S.V. Anisichkin, Patent 2269810; Ru, Composition for photosensitive layer of photomaterials, Bulletin of Invention 4 (12) (2006) (in Russia).
[10] A.V. Syui, D.S. Shtarev, Photosensitive composition based on polyvinyl alcohol, Optics and Spectroscopy 110 (2) (2011) 224–226.
[11] D.S. Shtarev, Photostimulated transformations in the polyvinyl alcohol–zinc oxide–bismuth chloride composition, Herald of the Far Eastern Branch of the Academy of Sciences 6 (148) (2009) 7–17 (in Russia).
[12] I.Yu. Prosanov, V.N. Brui, P.A. Babin, The X-ray diffraction analysis of the PVA–ZnO/TiO_2–$Pb(Ac)_2$ photosensitive composition, The Journal of the Science and Applied Photography 44 (2) (1999) 69–71 (in Russia).
[13] I.Yu. Prosanov, The influence of the vacuum heat on the photographic and fluorescence properties of the materials based on the PVA–ZnO composition, The Journal of the Science and Applied Photography 44 (2) (2001) 70–71 (in Russia).
[14] O.F. Sirets, V.V. Sviridov, V.G. Guslevich, The thermal transformations in PVA films containing the Fe III and Cu II chlorides, The Journal of the Science and Applied Photography 30 (2) (1985) 408–412 (in Russia).
[15] D.S. Shtarev, K.S. Makarevich, V.N. Brui, I.Yu. Prosanov, Photographic materials with direct blackening based on polymer–semiconductor compositions, in: Proceedings of the 4th Asia-Pacific Conference Fundamental Problems of Opto- and Microelectronics, Khabarovsk, Russia, 2004, pp. 398–400.
[16] I.Yu. Prosanov, Investigate the fluorescence and direct blackening in the PVA–ZnO–$Pb(CH_3COO)_2$ composition, The Journal of the Science and Applied Photography 48 (1) (2003) 67–69 (in Russia).
[17] I.Yu. Prosanov, The photoproceses in heterogeneous composition PVA–ZnO/TiO_2, Ph.D. thesis, Khabarovsk, 313, 2004 (in Russia).
[18] V.M. Grebenkina, A.L. Kartuzhansky, M.I. Kostenko, The nature of the photoactive absorption centers in PVA–Cu (II) chloride systems, The Journals of Applied Chemistry 5 (1990) 104–1080.
[19] D.S. Shtarev, The influence of the irradiation of the various spectral distribution on the polymer–semiconductor–salt of metal composition, in: IV-th International Optical Congress “Optics XXI-th century”. Conference “The Fundamental Problems of Optics”, St. Petersburg, 2006 (in Russia).

[20] D.S. Shtarev, The determination of the growth rate of the absorption bands under exposure of the polymer–semiconductor–salt of metal by the irradiation of the various spectral distribution, in: International Optical Congress “Optics XXI-th century”. Conference “The Fundamental Problems of Optics”, St. Petersburg, 2008 (in Russia).

[21] A.F. Holleman, E. Wiberg, Inorganic Chemistry, Academic Press, San Diego, 2001.

[22] D. Shindo, T. Oikawa, Analytical Electron Microscopy for Materials Science, Springer-Verlag, Berlin, 2002.

[23] C.A. Finch, Polyvinyl Alcohol—Developments, J. Wiley, 1992, 870 p.

[24] C.A. Finch, Polyvinyl Alcohol, Properties and application, J. Wiley, 1973, 339 p.

[25] B. Vincent Crist, Handbook of Monochromatic XPS Spectra, Semiconductors, Wiley, 2000, 568 p.

[26] B. Vincent Crist, Handbook of Monochromatic XPS Spectra, Polymers and Polymers Damaged by X-Rays, Wiley, 2000, 454 p.

[27] B. Vincent Crist, Handbook of Monochromatic XPS Spectra, the Elements of Native Oxides, Wiley, 2000, 548 p.

[28] NCBI Bookshelf, Polyene Antifungal Drugs, The University of Texas Medical Branch at Galveston, 1996 (retrieved 29 January 2010).

[29] O.V. Sverdlova, The Electron Absorption Spectrums in the Organic Chemistry, 2nd ed., Chemistry, Leningrad, 1985, 248 p. (in Russia).

[30] M. Matoumoto, K. Imai, Y. Kazuka, Journal of Polymer Science 28 (117) (1958) 426–428.

[31] M. Terazima, Molecular volume and enthalpy changes associated with irreversible photo-reactions, Journal of Photochemistry and Photobiology C: Photochemistry Reviews 3 (2) (2002) 81–108.

[32] L.I. Tarunina, F.O. Pozdnjakova, The Polymers Spectral Analysis, Chemistry, Leningrad, 1986, 248 p. (in Russia).

[33] T.A. Speranskaya, L.I. Tarunina, The Polymers Optical Properties, Chemistry, Leningrad, 1976, 136 p. (in Russia).

[34] M.C. Lee, W. Choi, Solid phase photocatalytic reaction on the soot/TiO_2 interface: the role of migrating OH radicals, Journal of Physical Chemistry B 106 (2002) 11818–11822.

[35] M.R.V. Sahyun, R. Brisbois, Photophysics of a particulate ZnO in organic dispersions: role of adsorbed carboxylate species, Electrochimica Acta 31 (1986) 19–24.

[36] D.H. Zhang, Fast photoresponse and the related change of crystallite barriers for ZnO films deposited by RF sputtering, Journal of Physics D: Applied Physics 6 (28) (1995) 1273.

[37] W. Wu, S. Bai, N. Cui, F. Ma, Z. Wei, Y. Qin, E. Xie, Increasing UV photon response of ZnO sensor with nanowires array, Science of Advanced Materials 2 (2010) 402–406.

[38] J. March, M.B. Smith, March’s Advanced Organic Chemistry: Reactions, Mechanisms and Structure, 5th ed., 2001.

[39] T.H. Lowry, K.S. Richardson, Mechanism and Theory in Organic Chemistry, 3rd ed., 1987.

[40] P. Sykes, Guidebook to Mechanism in Organic Chemistry, 6th ed., 1996.

[41] A. Wosylus, S. Hoffmann, M. Schmidt, M. Ruck, In-situ study of the solid–gas reaction of $BiCl_3$ to BiOCl via the intermediate hydrate $BiCl_3{\cdot}H_2O$, European Journal of Inorganic Chemistry 2010 (10) (2010) 1469–1471.

[42] N.N. Greenwood, A. Earnshaw, Chemistry of the Elements, 2nd ed., Butterworth-Heinemann, Oxford, 1997, 572 p.

[43] P. Pradyot, Handbook of Inorganic Chemical Compounds, McGraw-Hill, 2003, 1086.

[44] R.J. Meier, B.J. Kip, A quantum chemical study of the degradation and the maximum polyene length in PVC, Polymer Degradation and Stability 38 (1) (1992) 69–84.

[45] K. Maruyama, Y. Kuramoto, Y. Tanizaki, Absorption coefficients of polyenes in heated poly(vinyl alcohol) film and distribution of polyenes formed by its photodegradation, Polymer 30 (8) (1989) 1419–1424.

[46] G. Dirks, A.L. Moore, Th.A. Moore, D. Gust, Light absorption and energy transfer in polyene-porphyrin esters, Photochemistry and Photobiology 32 (2) (1980) 277–280.

[47] J.N. Murrell, The Theory of the Electronic Spectra of Organic Molecules, Wiley, NY, 1963, 328 p.

[48] M. Tsuji, S. Huzinaga, T. Hasino, Bond alternation in long polyenes, Reviews of Modern Physics 32 (1960) 425–427.

[49] I.Y. Prosanov, A.A. Matvienko, Study of PVA thermal destruction by means of IR and Raman spectroscopy, Physics of the Solid State 52 (10) (2010) 2203–2206 (in Russia).

[50] I.Y. Prosanov, Research of the thermal decomposition of the polyvinyl alcohol with the metal compound additive by the Raman spectroscopy, Physics of the Solid State 53 (4) (2011) 824–827 (in Russia).

[51] A.R. Blythe, D. Bloor, Electrical Properties of Polymers, Cambridge University Press, London, 2005, 492 p.

[52] J.D. Roberts, M.C. Caserio, Basic Principles of Organic Chemistry, 2nd ed., W.A. Benjamin, Inc., 1977, 1596 p.

[53] M.B. Smith, J. March, March’s Advanced Organic Chemistry: Reactions, Mechanisms and Structure, 5th ed., Wiley, 2001, p. 2083.

[54] Anna K. Cederstav, Bruce M. Novak, Investigations into the chemistry of thermodynamically unstable species. The direct polymerization of vinyl alcohol, the enolic tautomer of acetaldehyde, Journal of the American Chemical Society 116 (1994) 4073–4074.